HHS Public Access

Author manuscript

*ACS Infect Dis*. Author manuscript; available in PMC 2019 May 11.

Published in final edited form as:

*ACS Infect Dis*. 2018 May 11; 4(5): 758–770. doi:10.1021/acsinfecdis.7b00085.

# Fucosylated molecules competitively interfere with cholera toxin binding to host cells

**Amberlyn M. Wands**[1], **Jakob Cervin**[2], **He Huang**[3], **Ye Zhang**[3], **Gyusaang Youn**[3], **Chad A. Brautigam**[4], **Maria Matson Dzebo**[5], **Per Björklund**[6], **Ville Wallenius**[6], **Danielle K. Bright**[7], **Clay S. Bennett**[7], **Pernilla Wittung-Stafshede**[5], **Nicole S. Sampson**[3], **Ulf Yrlid**[2], and **Jennifer J. Kohler**[1,*]

[1]Department of Biochemistry, 5323 Harry Hines Blvd., UT Southwestern Medical Center, Dallas, TX 75390-9038, United States

[2]Department of Microbiology and Immunology, Institute of Biomedicine, University of Gothenburg, SE-40530 Gothenburg, Sweden

[3]Department of Chemistry, 100 Toll Rd., Stony Brook University, Stony Brook, NY 11790-3400, United States

[4]Departments of Biophysics and Microbiology, 5323 Harry Hines Blvd., UT Southwestern Medical Center, Dallas, TX 75390-8816, United States

[5]Chalmers University of Technology, Department of Biology and Biological Engineering, SE-41296 Gothenburg, Sweden

[6]Department of Gastrosurgical Research and Education, Sahlgrenska Academy, University of Gothenburg, Sahlgrenska University Hospital/Östra, Gothenburg, Sweden

[7]Department of Chemistry, 62 Talbot Ave, Tufts University, Medford, MA 02155, United States

## Abstract

Cholera toxin (CT) enters host intestinal epithelia cells, and its retrograde transport to the cytosol results in the massive loss of fluids and electrolytes associated with severe dehydration. To initiate this intoxication process, the B subunit of CT (CTB) first binds to a cell surface receptor displayed on the apical surface of the intestinal epithelia. While the mono-sialoganglioside GM1 is widely accepted to be the sole receptor for CT, intestinal epithelial cell lines also utilize fucosylated glycan epitopes on glycoproteins to facilitate cell surface binding and endocytic uptake of the toxin. Further, L-fucose can competively inhibit CTB binding to intestinal epithelia cells. Here, we

*Corresponding author information: Jennifer J. Kohler (jennifer.kohler@utsouthwestern.edu).

*Author contributions:* AMW performed experiments with cell lines and JC performed experiments with primary cells. HH, YZ, and GY synthesized polymers and DKB synthesized colitose. CAB performed MST analysis and MMD performed ITC analysis. PB and VW performed surgeries. CSB, PW-S, NSS, UY, and JJK supervised research. AMW, JC, NSS, UY, and JJK designed experiments, analyzed data, and wrote the manuscript.

**Conflict of Interest**

The authors declare no competing financial interest.

Supporting Information

Colitose synthesis, polymer synthesis, ELISA assays for AAL binding, flow cytometry histograms for CTB and lectin (AAL, MAL I, SNA) binding, blocking of CTB binding by L-colitose, blocking of CTB binding by L-glucose, ITC measurement of GM1a titrated to CTB, parameters obtained from fitting of the ITC data, and blocking of CTB and AAL binding by ganglioside oligosaccharides

use competition binding assays with L-fucose analogs to decipher the molecular determinants for L-fucose inhibition of cholera toxin subunit B (CTB) binding. Additionally, we find that mono- and di-fucosylated oligosaccharides are more potent inhibitors than L-fucose alone, with the LeY tetrasaccharide emerging as the most potent inhibitor of CTB binding to two colonic epithelial cell lines (T84 and Colo205). Finally, a non-natural fucose-containing polymer inhibits CTB binding two orders of magnitude more potently than the LeY glycan when tested against Colo205 cells. This same polymer also inhibits CTB binding to T84 cells and primary human jejunal epithelial cells in a dose-dependent manner. These findings suggest the possibility that polymeric display of fucose might be exploited as a prophylactic or therapeutic approach to block the action of CT toward the human intestinal epithelium.

## Graphical Abstract

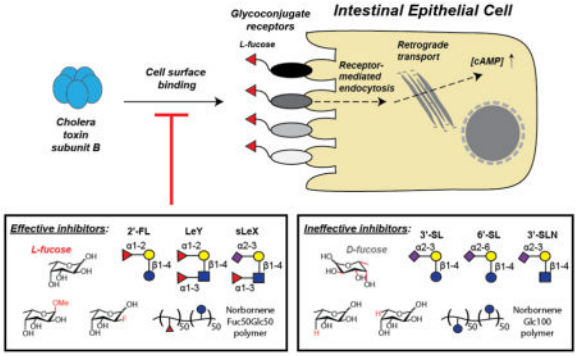


### Keywords

cholera toxin; fucose; human milk oligosaccharides (HMOs); ring-opening metathesis polymerization (ROMP); glycoproteins; gangliosides

Intestinal infection by the bacterium *Vibrio cholerae* is the cause of the diarrheal disease cholera. The required infectious dose is high and most patients are infected through contaminated drinking water or food that has been in contact with contaminated water. In endemic areas, young children are at highest risk for both infection and severe disease that can be life-threatening without proper treatment.[1] The reason for the higher sensitivity in children is most likely due to a lack of a sufficient immune response to recognize and combat the pathogen.[2] The standard treatment in the clinic is intravenous (IV) fluids initially to replace the lost water and to add nutrition. If the patient is not experiencing excessive vomiting then oral rehydration therapy (ORT) can be administered to speed recovery and decrease mortality. ORT can also be a first line treatment for patients with less severe symptoms. The infection can usually be cleared without antibiotics, but antibiotics can speed recovery and might be necessary in some moderate to severe cases to cure cholera.[3]

Cholera toxin (CT) is the main causative agent of cholera symptoms. CT consists of two different kinds of subunits, one enzymatically active A subunit and a pentameric ring formed of B subunits (CTB) responsible for cell surface binding. To exert its effects, CT must bind receptors presented on the surface of human intestinal epithelial cells, be internalized by the

formation of endocytic vesicles, and be released into the cytosol via retrograde transport through the Golgi to the endoplasmic reticulum (ER).[4] The A and B subunits separate in the ER and the A subunit moves to the cytoplasm where it activates Gαs, leading to production of cAMP. Accumulation of cAMP leads to unregulated ion secretion by the cells, which in turn gives rise to the diarrhea through osmotic effects.[5]

It has long been thought that the ganglioside GM1a is the main functional receptor for CT and therefore the GM1a-CTB interaction has been well studied.[6,7] For example, addition of exogenous GM1a to the rabbit ileum increased sensitivity to CT in a dose-dependent manner.[8] Furthermore, the high affinity binding of GM1a by CTB (as compared to other possible lower affinity glycolipid or glycoprotein candidates) certainly points in favor of GM1a being the main receptor. Substantial data detailing GM1a-dependent trafficking of CT demonstrate that GM1a is capable of functioning as a CT receptor.[9–11] The extensive characterization of CTB-GM1a recognition has spurred efforts to design molecules that competitively interfere with CTB binding to GM1a. For example, Yu *et. al.* recently described the blocking of CTB binding to GM1a using tailored peptides, with $IC_{50}$-values in the nM range.[12] Using the colonic cell line Caco-2, they demonstrated that such peptides can interfere with CT function at a cellular level. Because CTB forms a pentamer, multivalent display of competitive ligands has been used to achieve more potent inhibitors.[13,14] In a recent example of this strategy, a pentameric glycocluster consisting of the GM1a oligosaccharide linked to a calixarene macrocycle was shown to inhibit CTB binding at picomolar concentrations *in vitro*.[15] However, experiments to evaluate such reagents typically assess affinity for CTB or ability to block CTB binding to purified gangliosides, but often do not assess effects on CTB binding cell surfaces that express receptors other than GM1a.[16–20] A notable exception is recent work by Pieters and colleagues in which molecules displaying multiple copies of the GM1a oligosaccharide were shown to protect human intestinal organoids from CT-induced swelling.[21]

While GM1a-based molecules can be potent blockers of CTB binding and CT action, several studies suggest that human intestinal cells have only low amounts of GM1a on the surface.[8,22] These low levels of GM1a, together with the possibility that other molecules may also bind CTB, raised the prospect that other CTB binding cell surface molecules might function as CT receptors in CT-induced host cell intoxication. Indeed, we recently found that the rat C6 glioma cell line, deficient in GM1a but abundant in GM3, shows a marked increase in sensitivity to CT when treated with a small molecule inhibitor to block glucosylation of ceramide (an early step in glycosphingolipid biosynthesis).[23] In this same work, we observed that B4galnt1-deficient mice, which lack GM1a, exhibit an enhanced secretory response to CT as compared to wild-type mice. These results imply that molecules other than GM1a may function as CT receptors *in vivo*.

Studies from our groups and others have provided insight into the nature of non-GM1a receptors for CT. Biochemical and structural studies have demonstrated that fucosylated glycans, including human milk oligosaccharides (HMOs) and blood group antigens (BGAs), can bind to CTB.[24–29] Cell-based experiments performed with human colonic epithelial cell lines and primary intestinal cells identified a role for fucosylated glycoconjugates in mediating CTB binding to the cell surface.[23,30] These findings led us to further investigate

how fucose interacts with CTB and affects CTB binding to host cells. Here we describe the use of cell-based competition assays to perform a structure-activity relationship (SAR) analysis of the CTB-fucose interaction. Using the same experimental approach, we also evaluated the ability of small fucosylated glycans to interfere with host cell binding by CTB. The results of these experiments provide insight into the fucose linkage and underlying glycan structure preferentially recognized by CTB. With this detailed knowledge in hand, we proceeded to use polymeric display of fucose to develop novel and potent CTB blockers.

## Results and Discussion

Having previously observed that L-fucose can competitively interfere with CTB binding to host cells,[23,30] our goal in this work was to identify the molecular features of L-fucose that allow it to function as a competitive inhibitor of CTB binding and to use that knowledge to create molecules that more potently block CTB binding to host cells. In considering our goal, as well as recent evidence that CTB may have more than one glycan binding site,[25] we chose to employ competitive binding assays that measure CTB binding to host cell surfaces, rather than CTB binding to a single glycan ligand. Four major aspects were imbedded into the design of our structure-activity relationship (SAR) approach (Figure 1). Briefly, candidate inhibitors were first screened at a single dose of toxin and single dose of inhibitor against a single target cell line to identify structural changes that reduce the effectiveness of L-fucose as an inhibitor. These results were then validated against an additional target cell line by the ability of the inhibitors to suppress binding of multiple concentrations of CTB. Inhibitors that appeared most potent in these initial screening assays were subjected to quantitative comparison by determination of IC50 values for inhibition of CTB binding. Finally, the most potent inhibitors were evaluated for physiological relevance by assessing whether they could inhibit CTB binding to human jejunal primary epithelial cells.

First, we investigated the stereochemical basis of L-fucose inhibition of CTB binding. We utilized the enantiomer of L-fucose (*i.e.*, D-fucose) and a diastereomer 6-deoxy-D-glucose (Figure 2a), both of which are predicted to have the same or similar hydrophobicity properties as L-fucose, yet contain altered spatial patterning of hydroxyl groups. We used two assays we developed previously, in which we evaluate the ability of monosaccharides and other molecules to competitively interfere with lectin and CTB-biotin binding to the surface of two intestinal epithelial cell lines (Colo205 and T84 cells).[30] For Colo205 cells, lectin and CTB-biotin binding was measured by flow cytometry, using dichlorotriazinylamino fluorescein (DTAF)-conjugated streptavidin as a detection reagent. For T84 cells, lectin and CTB-biotin binding was measured by ELISA assay, using HRP-streptavidin and ortho-phenylenediamine (OPD) for detection. As expected, L-fucose could effectively block binding of the positive control L-fucose-specific *Aleuria aurantia* lectin (AAL) to either Colo205 or T84 cells, while D-fucose and 6-deoxy-D-glucose had virtually no effect (Figure S1). When these monosaccharides were assayed at a 100 mM concentration for their ability to inhibit CTB binding to Colo205 cells, only L-fucose served as an effective inhibitor, reducing toxin binding to ~20% of the no sugar control; in contrast, both D-fucose and 6-deoxy-D-glucose had only minor effects on CTB binding (Figure 2b). Similar inhibitory trends were observed when these monosaccharides were assayed for their ability to block CTB binding to T84 cells, in which the dose-dependent increase in cell

surface CTB binding was monitored. Only inclusion of 200 mM L-fucose could dramatically suppress CTB binding to T84 cells, with D-fucose producing only a modest effect, and 6-deoxy-D-glucose had no effect (Figure 2c). Overall, these data indicate that the L-fucose-CTB interaction is specific and dependent on the stereochemical positioning of the hydroxyl groups.

Next, we probed whether the anomeric position of L-fucose contributes to CTB recognition. First, we locked the hydroxyl group on the anomeric carbon (position 1) in either the α- or β-conformation by the addition of a methyl group (Figure 3a). When tested against Colo205 cells at 100 mM concentrations, methyl α-L-fucose inhibited CTB binding as efficiently as L-fucose, while the inhibitory potential of the methyl β-L-fucose was significantly less (Figure 3b). Similarly, for T84 cells, suppression of CTB binding was observed with either 200 mM L-fucose or methyl α-L-fucose, but inhibitory activity was not observed for methyl β-L-fucose (Figure 3c). In addition, the α-anomer of fucose was slightly more effective at inhibiting cell surface binding of AAL than the β-anomer was (Figure S4). Overall, these data support the idea that an L-fucose residue displayed in an α-linkage can be accommodated into the binding pocket(s) of CTB.

We then examined the roles of hydroxyl groups at the 2, 3, or 4 positions by assaying the inhibitory activities of 2-deoxy-2-fluoro-L-fucose (Figure 3a), L-colitose (Figure S5), and 4-deoxy-L-fucose (Figure 3a), respectively. When tested as CTB inhibitors against either Colo205 or T84 cells, 2-deoxy-2-fluoro-L-fucose and L-fucose were indistinguishable (Figures 3d and 3e). With a C–F bond serving as an isosteric substitution for a C–O bond,[31] this result suggests that the hydroxyl group at C-2 does not contribute significantly to the CTB-fucose binding interaction as a hydrogen bond donor. In addition, due to the highly polarized nature of the newly introduced C–F bond, the fluorine atom has a ~75% reduced ability to serve as a hydrogen bond acceptor,[31] and thus it is unlikely that the hydroxyl group at the C-2 position contributes significantly to the CTB-fucose binding interaction as a hydrogen bond acceptor. In contrast, removal of the hydroxyl group at the 3-position (*i.e.*, L-colitose) led to a significant loss in inhibitory potential towards CTB binding when tested at a 200 mM concentration against T84 cells (Figure S5), and removal of the 4-position hydroxyl group (4-deoxy-fucose) resulted in a complete loss in inhibitory potential towards CTB binding against both Colo205 cells (Figure 3d) and T84 cells (Figure 3e). We note that 4-deoxy-fucose cannot adopt a furanose form, and that colitose exists primarily in the pyranose forms.[32] Therefore, it is reasonable to interpret the reduction in blocking ability as indicating that the hydroxyl groups at positions C-3 and C-4 could serve as important hydrogen bonding donors or acceptors within the CTB-fucose binding interaction. Taken together, these data indicate a trend for free L-fucose binding to CTB in which the importance of the contacts made are position 4 > position 3 > position 2. However, it is worthwhile to note that these SAR studies were performed with free sugars, rather than glycosides. Therefore, effects on either the conformation or the open-chain/hemiacetal equilibrium of the sugar could also contribute to the observed reduction in inhibitory activity.

Finally, we looked at the effect of modifying the methyl group at position 6, either by the addition of a hydroxyl group (*i.e.*, L-galactose) or by its removal (*i.e.*, D-arabinose) (Figure

3a). When tested against both Colo205 and T84 cells, we observed that both L-galactose and D-arabinose can function as effective inhibitors of AAL cell surface binding, with an order of potency as follows: L-fucose > L-galactose > D-arabinose (Figure S6). We next wanted to determine if these trends hold true for inhibition of CTB as well, to gain insight into that specific region of the CTB binding pocket being utilized by L-fucose. In this regard, we observed that CTB can tolerate the addition of a hydroxyl group to the C-6 methyl group (*i.e.,* L-galactose) with modest loss in inhibition against binding to either Colo205 or T84 cells (Figures 3f and 3g). We also observed that combining hydroxylation of the C-6 methyl group with inversion of the stereochemistry at C-4 (*i.e.* L-glucose), results in a loss of all inhibitory activity (Figure S7); this is consistent with the loss in activity we observed with removal of the C-4 hydroxyl group (*i.e.*, 4-deoxy-L-fucose) (Figures 3d and 3e). Interestingly, removal of the methyl group at C-5 (*i.e.,* D-arabinose) revealed differences between the specificities of the CTB and AAL binding pockets. Unlike AAL, which could accept D-arabinose as an effective inhibitor of cell surface binding (Figure S6), D-arabinose performed indistinguishably from the no sugar control when tested against CTB binding to both Colo205 and T84 cells (Figures 3f and 3g). This result implies that the methyl functional group at position 6 plays a critical role in the specific recognition of L-fucose by CTB, possibly through an interaction with key hydrophobic residues within the CTB binding pocket.

With the knowledge that L-fucose makes specific spatial and positional contacts within the CTB binding pocket(s), we next compared the inhibitory activity of small glycans, some of which included L-fucose. Human milk oligosaccharides (HMOs) are studied for their therapeutic benefits in human milk,[33,34] and thus we were able to acquire a small panel of lactose-based glycans with either an L-fucose or sialic acid modification (Figure 4a). When assayed against Colo205 cells at a 100 mM concentration, we observed that the non-fucosylated lactose inhibited CTB binding by ~50 %. However, when L-fucose was attached in an α-1-2 linkage to the galactose residue (*i.e.*, 2′-fucosyllactose or 2′-FL), the glycan now functioned as a more potent inhibitor than L-fucose alone; in contrast, 3-fucosyllactose (3-FL), in which L-fucose is displayed in an α-1-3 linkage from the glucose residue of the lactose backbone, displayed inhibitory activity comparable to L-fucose alone (Figure 4b). We also confirmed that 2′-FL functions as a more potent inhibitor against CTB cell surface binding than the L-fucose monosaccharide when tested against T84 cells at a 100 mM concentration (Figure 4c). However, when sialic acid was displayed in either an α-2-3 linkage (3′-sialyllactose or 3′-SL) or α-2-6 linkage (6′-sialyllactose or 6′-SL) from the galactose residue of lactose, no inhibition of CTB cell surface binding was observed against either Colo205 cells (Figure 4b) or T84 cells (Figure 4c). Furthermore, non-fucosylated lactose did not inhibit CTB binding to T84 cells (Figure 4c), indicating that modification by L-fucose is a more general requirement for inhibition of CTB binding across different intestinal epithelial cell lines. To ensure that these glycans of interest were in fact being assayed at an effective concentration, we confirmed the abilities of 2′-FL and 3-FL to inhibit binding of the *Aleuria aurantia* lectin (AAL) against Colo205 cells, as well as α-2-3 sialyated lactose to enhance the inhibitory potential of lactose against *Maackia amurensis* lectin I (MAL I) and α-2-6 sialylated lactose to enhance the inhibitory potential of lactose against *Sambucus nigra* lectin (SNA) (Figure S9). Taken together, these data indicate that

fucosylated, rather than sialylated, HMOs can serve as effective inhibitors of CTB binding to intestinal epithelial cell lines. While our previous studies suggested that sialic acid could inhibit CTB binding to both Colo205 and T84 cells,[30] these new data reveal that those results may have been an artifact resulting from a high concentration of sialic acid that reduced the pH of the solution to a point at which CTB became denatured (Figure S10).[35]

Starting with the most potent ligand identified thus far, 2′-FL, we tested whether additional modifications to the oligosaccharide could increase blocking efficacy. Work by the Krengel lab utilizing both NMR and x-ray crystallographic techniques has shown that Lewis Y (LeY), which is structurally similar to 2′-FL, can bind to a novel binding pocket on CTB,[25,26] and recent glycan array data show that CTB can recognize LeY-containing glycans.[29] We therefore took a stepwise approach originating from 2′-FL and ending at the A and B blood group variants of LeY (Figure 5a) to identify more potent ligands that block CTB binding to Colo205 cells. We started by either adding an α1-3 fucose (creating difucosyllactose, or DF-L) or by changing the Glc to a GlcNAc residue (creating H antigen). When assayed at 10 mM (a 10-fold lower concentration than used in previous experiments), all three glycans (*i.e.,* 2′-FL, DF-L, and H antigen) performed indistinguishably, reducing CTB binding by at least 75% compared to the no sugar control, and thereby serving as more potent CTB inhibitors than either L-fucose alone or the corresponding non-fucosylated disaccharides (*i.e.* lactose and LacNAc) (Figure 5b). Combining both of the aforementioned modifications simultaneously onto 2′-FL creates LeY or Fucα2Galβ4[Fucα3]GlcNAc (Figure 5a). LeY was identified as the most potent blocker when assayed at 10 mM, performing significantly better than 2′-FL, DF-L and H antigen (Figure 5b). This suggests involvement of both the α1-3 fucose and the acetyl amine group of GlcNAc in stabilizing or facilitating the binding to CTB, consistent with contacts observed in the crystal structure of CTB-LeY.[25] Since blocking with LeY was quite potent at 10 mM, further analysis of LeY variants was performed at 1 mM. For example, addition of Gal or GalNAc to the LeY Gal residue introduces the B and A blood group antigens (creating BLeY and ALeY, respectively) (Figure 5a). Addition of either of these BGAs to the LeY tetrasaccharide core failed to produce a further increase in potency for blocking of CTB binding to Colo205 cells (Figure 5c). Interestingly, blocking of AAL binding to Colo205 cells was more efficient with the difucosylated ligands (*i.e*, DF-L and LeY) than with monofucosylated ligands (*i.e.*, 2′-FL and H antigen) when tested at either 10 mM (Figure S12) or 1 mM (Figure S13) concentrations. Further, when GalNAc or Gal was added to the LeY tetrasaccharide, forming the A and B blood group antigens, we observed a less efficient blocking of AAL binding (Figure S13).

To evaluate whether the blocking of cell surface CTB by binding by low millimolar concentrations of LeY could indeed be caused by a direct binding interaction between the CTB and the LeY tetrasaccharide, we turned to isothermal titration calorimetry (ITC) and microscale thermophoresis (MST) methods to evaluate protein-glycan binding. The result from ITC analysis showed that LeY binds to CTB with a $K_D$ of 1.4 mM (Figure 5d), which agrees with the previously reported value of 1.8 mM for the binding of a slightly modified LeY to El Tor CTB.[24] Similar values have also been determined using surface plasmon resonance (SPR).[25] The affinity of LeY to CTB is indeed weaker than the well-known interaction of GM1 to CTB, which has a $K_D$ in the nM range (consistent with the inhibitory

concentration observed in this study, see Figure S14).[7] We confirmed our ITC results using an additional method, MST. In the MST analysis, the changes in thermophoresis as a function of concentration could be fitted to a 1:1 binding model, resulting in a $K_D$ of 4 mM (68.3% confidence interval is 2 – 14 mM) (Figure 5e). Thus, the observed inhibition of CTB binding by LeY can reasonably be attributed to a direct interaction between CTB and LeY.

Having observed that 2′-FL can be converted to a more potent CTB inhibitor (*i.e.* LeY) by modification of the glucose residue with both a C2 *N*-acetyl group and a C3 fucosyl residue, we wondered whether the same modifications could be used to convert an inactive ligand, such as 3′-SL, into an effective inhibitor of CTB binding (Figure 6a). In fact, when assayed against Colo205 cells at a 1 mM concentration, *N*-acetylated 3′-SL (*i.e.* sialyl LacNAc, or 3′-SLN) was incapable of inhibiting CTB cell surface binding (Figure 6b). However, under the same assay conditions, when *N*-acetylation of C2 was performed in combination with fucosylation of C3 on the glucose residue of 3′-SL to produce sialyl LeX (sLeX), this ligand possessed an inhibitory potential only 2-fold less than that of LeY (Figure 6b). An analogous experiment performed against AAL yielded different results, in which incubation with sLeX retained ~70% of the lectin bound to the cell surface, as opposed to the ~15% achieved by incubation with LeY (Figure S16). These data illustrate an interesting difference in the binding profile of the glycan epitopes that can be accommodated by the CTB and AAL binding pockets; while both lectins prefer the difucosylated ligand, only CTB is able to tolerate substitution of the α-1-2 fucose with an α-2-3 sialic acid with minimal loss in inhibitory potential.

We then further characterized the dose-dependent inhibitory activity of key molecules identified in this study, from which a clear trend in inhibitory potential of LeY > sLeX > 2′-FL > L-fucose was observed for CTB binding to both Colo205 cells (Figure 6c) and T84 cells (Figure 6d). With regards to Colo205 cells (Figure 6c), L-fucose possesses an $IC_{50}$ value of 14.5 mM ± 0.8 mM against CTB binding, which can be further reduced by ~5-fold by positioning the L-fucose in an α-1-2 linkage to the galactose residue of a lactose scaffold (*i.e.* 2′-FL). Upon conversion of 2′-FL to LeY by two key structural changes described previously, this inhibitory potential can be enhanced by an additional order of magnitude (from $IC_{50}$ = 3.0 mM ± 0.7 mM for 2′-FL to $IC_{50}$ = 0.24 ± 0.05 mM for LeY).

Finally, we evaluated the ability of LeY to block CTB binding to human jejunum primary epithelial cells, which are believed to the primary physiological site of CT action. Cells were isolated from human jejunal tissue donated from patients undergoing a gastric bypass procedure. Single cell suspensions were stained and gated for $EpCAM^+$ and CD45-negative to identify epithelial cells and to study how they bound CTB using flow cytometry. Similar to results with Colo205 cells (Figures 6c), the LeY glycan was also able to effectively block CTB binding to human jejunum primary cells in a dose-dependent manner when titrated from 0.1 – 1 mM, and with a potency greater than that of 2′-FL (Figure 6e). Furthermore, no inhibition of CTB binding to these primary epithelial cells was observed with the non-fucosylated LacNAc control when tested at 5 mM (Figure 6e). Thus, the inhibitory trends observed in human colonic epithelial cell lines also hold true in primary human jejunal epithelial cells.

We also wished to compare the inhibitory potential of LeY to previously characterized competitive inhibitors of CTB binding derived from the glycolipids asialo-GM1 and GM1a (Figure S18a). We observed that the oligosaccharide headgroup from GM1a, GM1a(os), competitively inhibits CTB binding to two different colonic epithelial cell lines (*i.e.* Colo205 and T84) with considerably different efficiencies. For instance, when GM1a(os) and LeY were both assayed at a 1 mM concentration against Colo205 cells, GM1a(os) displayed the most potent inhibition of CTB binding, reducing CTB binding down to ~5% of the no sugar control as compared to ~20% exhibited by LeY (Figure S18b). Upon removal of the sialic acid modification from GM1a(os) to create GA1(os), the inhibitory potential was significantly attenuated (Figure S18b), thus consistent with the "two-fingered grip" mechanism of binding utilized by GM1a.[6,7] As a control we verified that only the fucosylated oligosaccharide LeY, and not GA1(os) or GM1a(os), were capable of inhibiting AAL cell surface binding when assayed at 1 mM (Figure S18c). When we further assayed the ability of the GM1a(os) pentasaccharide to function as a CTB inhibitor against Colo205 cells in a dose-dependent manner, it was found to possess an $IC_{50}$ value of 109 ± 38 nM, which is approximately 2000-fold more potent than that of the LeY tetrasaccharide (Figure S18d). On the contrary, when assayed against T84 cells, although a decrease in CTB binding was observed in the presence of as little as 100 μM GM1a(os), this glycan could not completely inhibit CTB binding, even with as much as 10 mM GM1a(os) added (while the addition of GA1(os) resulted in no inhibition), consistent with similar observations that we have made using primary human intestinal epithelial cells.[23] This observation with the GM1a(os) contrasts with the near complete inhibition observed for CTB binding to T84 cells upon inclusion of either 5 mM LeY or 10 mM sLeX (Figure S19). Overall, these data indicate that LeY, not GM1a(os), is a common ligand that inhibits well across both Colo205 and T84 cells, while the potency of the GM1a(os) as a CTB inhibitor is cell line-dependent.

Having observed that the difucosylated structure LeY was the most effective inhibitor of CTB binding across both colonic epithelial cell lines, we next tested whether a fucose-based polymer could increase blocking further. We envisioned that polymeric display of fucose would increase avidity toward the CTB pentamer and could potentiate aggregation of CTB to more efficiently block binding to the intestinal epithelium. Indeed, recent glycan array data indicate that CTB can bind biantennary, fucosylated HMOs. [29] We tested a polymer composed of a norbornene backbone of about 100 monomer units in length and displaying a random mixture of fucose and glucose (poly($NBFuc_{50}$-*ran*-$NBGlc_{50}$), abbreviated Fuc50Glc50 here). A glucose-only polymer (poly$(NBGlc)_{100}$, abbreviated Glc100) was used as a control (Figure 7a). A titration of the ability of polymers to block CTB binding to Colo205 cells yielded an $IC_{50}$ = 1.5 ± 0.9 μM for Fuc50Glc50, with no significant inhibitory effect of Glc100 even up to 25 μM (Figure 7b). Thus, the polymer is about 150–200 times more effective at inhibiting CTB binding compared to LeY, and about 10,000 times more effective than free fucose (Figure 7b and 6c). Calculated on a ligand (fucose) basis, polymeric display of fucose yields a 200-fold enhancement in inhibitory activity as compared to free fucose and a 3- to 4-fold enhancement relative to LeY. Polymer blocking activity is also similar across intestinal epithelial cells: Fuc50Glc50 displayed dose-dependent blocking of CTB binding to both T84 cells (Figure 7c) and primary human

jejunal epithelial cells (Figure 7d), while a less dramatic effect (if any) was observed for the Glc100 control.

Collectively, our competitive binding studies indicate that the Fuc50Glc50 polymer can potently block CTB binding when utilized at micromolar concentrations, as compared to the millimolar concentrations that would be required by either free fucose or small fucosylated glycans to give similar results. A water-soluble reagent like the norbornene polymer evaluated here could potentially be added to drinking water or food. Hence, the therapeutic potential for a L-fucose-based polymer may be a promising complement to the current treatment of oral isosmotic fluid. One can also speculate that this kind of reagent might be used prophylactically in situations with elevated risk of *V. cholerae* infection. Further, fucose-based reagents also have the potential to interfere with *V. cholerae* adherence to the intestinal lining.[36] We will continue to test this and other fucose-based polymers in vitro and in vivo to further characterize their potentials for therapeutic and prophylactic treatment of cholera.

To summarize, we have characterized the ability of L-fucose to block CTB binding to multiple intestinal epithelial cell lines. The results of these experiments provide a better understanding of how L-fucose interacts with CTB in solution and how using fucosylated glycans or polymers can increase the blocking effect. While free L-fucose bound by CTB has not been characterized structurally, a crystal structure has been solved of CTB bound to the LeY tetrasaccharide via a binding site located auxiliary to the canonical GM1a binding site.[25] However, because T84 and Colo205 cells were both previously reported to express low levels of GM1a similar to that found in the human intestine,[8,22,30] the ability of the GM1a(os) to exert any inhibitory effect against CTB binding to these cell lines suggests that fucosylated glycans displayed on cell surfaces may bind CTB competitively with GM1a. One explanation could be that fucosylated cell surface glycoproteins could be targeting CTB through both the newly discovered auxiliary binding site as well as the canonical GM1a binding site (albeit with a lower affinity than can be achieved through GM1a binding), thus partially overlapping with the contacts required for GM1a(os) inhibitor binding. In relation to this idea, we speculate that the monolayers of T84 cells used in the ELISA binding assays reported here may possess more fucosylated glycoprotein receptors on their cell surface than the isolated and spherical Colo205 cells utilized in the flow cytometry assay. Such a difference could explain why CTB binding to T84 cells is less responsive to competitive inhibition by the GM1a(os). Along those lines, we recently reported that GM1a-deficient C6 glioma cells treated with a sialyltransferase inhibitor exhibited a marked increase in the abundance of terminal galactose-containing glycans located on glycoproteins as determined by a peanut agglutinin (PNA) lectin blot, as well as an enhanced sensitivity to CT intoxication as measured by cAMP accumulation.[23] Additionally, we observed that pretreatment of human jejunal tissue with either AAL (fucose-recognizing) or PNA (galactose-recognizing) lectin could block CT-induced $Cl^-$ secretion in an Ussing chamber experiment.[23] Collectively, these data suggest that the differential abundance among cell lines of terminal galactose residues present on glycoproteins could play a role in their sensitivity to CTB blocking by the GM1a oligosaccharide. More research is needed to distinguish between these and other possible explanations.

Both epidemiological and biochemical data indicate that CT can distinguish between ABO blood group antigens, with the El Tor variant of CTB exhibiting stronger discriminatory ability than the classical variant.[24,25,37] Similarly, the experiments reported here show that ALeY blocks CTB binding to Colo205 cells less effectively than LeY does. We also observed that BLeY displayed comparable blocking activity as LeY (Figure 5c). This suggests that the aminoacetyl group on GalNAc interferes with binding to CTB while the Gal residue alone can be accommodated into the glycan binding pocket. We note that Colo205 cells are type H(O) and therefore would not express the ALeY and BLeY antigens on their cell surfaces. [38] Therefore, it would be interesting to investigate whether cell lines expressing A or B antigens yield similar results. Furthermore, our observation that the sLeX blood group antigen can also serve as an inhibitor of CTB binding provides insight as to why we were previously able to utilize a metabolically incorporated sialic acid photocrosslinking sugar (*i.e.* SiaDAz) to covalently capture its glycoprotein binding partners in both Colo205 and T84 cells.[30] Further, this result may explain why the functional receptor for CT might have been elusive in those studies due to the limitation of relying on SiaDAz to capture the complete array of fucosylated (and possibly not sialylated) glycan binding partners.

The inhibition observed with 2′-FL is intriguing; while not a particularly potent CTB inhibitor, its activity has potential physiological relevance. Indeed, 2′-FL can be detected in human milk at approximately 4 mM,[39,40] which is similar to the $IC_{50}$ value observed for 2′-FL against CTB binding to Colo205 cells. Comparing human and bovine milk, human milk contains more oligosaccharides and the oligosaccharides present in human milk are predominately fucosylated (50–80%). However, in bovine milk, the oligosaccharides are predominately sialylated and only a small fraction fucosylated.[41] This clear difference suggests a species-dependent importance of the HMO composition. While human milk is known to protect infants from diarrheal disease, this effect has historically been attributed to maternal antibodies in the milk. However, an emerging body of literature indicates that HMOs – specifically α-1-2-fucosylated glycans – protect infants against diarrheal diseases of multiple etiologies.[33,34] Here we show that 2′-FL can inhibit CTB binding. Future studies will test whether 2′-FL blocks the action of additional enteric bacterial toxins, such as the heat-labile enterotoxin (LT) from *E. coli*, whose mature B subunit (LTB) shares 83% identity with CTB and also causes severe diarrheal disease.[42]

Finally, we show that a water-soluble fucosylated polymer, utilized at micromolar concentrations, can inhibit CTB binding to both cultured and primary intestinal epithelial cells. Although many previous studies have been conducted using GM1-based polymers and multimers to block CTB binding, this is the first report that fucosylated polymers can efficiently block CTB binding to human cells, consistent with previous studies that indicate that CTB utilizes binding partners other than GM1.[23,25,30,43–49] If effective in humans, a fucose-based polymer approach would have the potential to complement existing therapies and might also be useful as a prophylactic in populations at high risk for cholera.

# Methods

## General

**Chemicals—**Bovine serum albumin (BSA, Fraction V, heat shock treated) was purchased from both Fisher (catalog no. BP1600) and Sigma (catalog no. A9647). Dichlorotriazinylamino fluorescein (DTAF) streptavidin was purchased from Jackson ImmunoResearch (catalog no. 016-010-084). PureCol bovine collagen solution was purchased from Advanced BioMatrix (catalog no. 5005-B). Paraformaldehyde (formaldehyde) aqueous solution (20%) was purchased from Electron Microscopy Sciences (catalog no. 15713). Streptavidin-POD conjugate was purchased from Roche (catalog no. 11089153001). *ortho*-Phenylenediamine dihydrochloride (OPD) was purchased from Sigma (catalog no. P1526). Acetoxyacetic acid was purchased from Sigma (99% pure) (catalog no. 302341). Sodium bicarbonate was purchased from ACROS Organics (≥ 99.7% pure) (catalog no. 424270251).

**Carbohydrates—**The following reagents were purchased from Sigma (St. Louis, MO): l-(−)-Fucose (≥ 99% pure) (catalog no. F2252), d-(+)-Glucose (≥ 99.5% pure) (catalog no. G7021), d-(+)-Fucose (≥ 98% pure) (catalog no. F8150), d-(−)-Arabinose (≥ 98% pure) (catalog no. A3131), l-(+)-Arabinose (≥ 99% pure) (catalog no. A3256), d-Lactose monohydrate (≥ 99.5% pure) (catalog no. 61339). The following reagents were purchased from Carbosynth (Berkshire, UK): 6-deoxy-D-glucose (min 98% pure) (catalog no. MD04994), Methyl a-L-fucopyranoside (min 98% pure) (catalog no. MM02387), Methyl b-L-fucopyranoside (min 98% pure) (catalog no. MM05588), 2-Deoxy-2-fluoro-L-fucose (min 98% pure) (catalog no. MD06089), L-colitose (min 95% pure) (catalog no. MC71709), 4-Deoxy-L-fucose (min 98% pure) (catalog no. MD03942), L-Galactose (min 99% pure) (catalog no. MG05473), N-Acetyl-D-lactosamine (min 98% pure) (catalog no. OA08244), 2′-Fucosyllactose (min 95% pure) (catalog no. OF06739), 3-Fucosyllactose (min 98% pure) (catalog no. OF05673), 3′-Sialyllactose sodium salt (min 98% pure) (catalog no. OS04397), 6′-Sialyllactose sodium salt (min 98% pure) (catalog no. OS04398), *N*-Acetylneuraminic acid (min 98% pure) (catalog no. MA00746), 3′-Sialyl-N-acetyllactosamine (min 95% pure) (catalog no. OS00732), 3′-Sialyl Lewis X (min 95% pure) (catalog no. OS04058), Asialo-GM1-tetrasaccharide (min 90% purity) (catalog no. OG03927). The following reagents were purchased from Elicityl (Crolles, FR): Blood group H antigen triaose type 2 (>50% purity) (catalog no. GLY031-2), Difucosyllactose (>90% purity) (catalog no. GLY066), Lewis Y (LeY) tetraose (> 90% purity) (catalog no. GLY048), Blood group A Lewis Y antigen pentaose type 2 (min >90% purity) (catalog no. GLY035-5), Blood group B Lewis Y antigen pentaose type 2 (min >90% purity) (catalog no. GLY038-5), GM1a ganglioside sugar (> 90% purity) (catalog no. GLY096). Colitose was also prepared synthetically as described in the Supporting Information.

**Polymers—**Synthesis procedures for the polymers can be found in the Supporting Information.

## Cell culture

The following reagents for general cell culture use were purchased from Thermo Fisher Scientific/Gibco: penicillin-streptomycin (catalog no. 15140), fetal bovine serum (FBS) (catalog no. 16000), TrypLE express enzyme with phenol red (catalog no. 12605), and distilled water (catalog no. 15230). Dulbecco's Phosphate Buffered Saline (DPBS) was purchased from Sigma (catalog no. D8537). Colo205 cells (ATCC) were maintained in RPMI 1640 medium supplemented with 2 mM L-glutamine, 10 % (v/v) FBS, and penicillin-streptomycin. T84 cells (ATCC) were maintained in DMEM/F-12 medium supplemented with 2.5 mM L-glutamine, 15 mM HEPES (Gibco, catalog no. 11330), 5 % (v/v) FBS, and penicillin-streptomycin. T84 cells were not used past passage number 45. All cell lines were maintained at 37 °C, 5 % carbon dioxide in a water-saturated environment. The Countess automated cell counter (Thermo Fisher Scientific/Invitrogen) was used for cell counting.

## Flow cytometry

Colo205 cells were harvested from 10 cm tissue culture plates seeded at either 2 million cells/10 mL and cultured for 2 d or 1 million cells/10 mL and cultured for 3 d. Colo205 cells were removed from the tissue culture plate by adding 1.5 mL of trypsin for 2 min at 37 °C, pelleted by centrifugation, resuspended in DPBS, and ~350,000 cells in 200 μL were transferred per well of a v-bottom 96-well plate (Corning, catalog no. 3897). Cells were washed twice with 200 μL cold DPBS containing 0.1% (w/v) BSA, then incubated 30 min on ice with 50 μL (10 μg/mL) of biotin-conjugated cholera toxin subunit B (CTB) (Thermo Fisher Scientific/Invitrogen, catalog no. C-34779) diluted in DPBS/BSA containing the indicated concentrations of free carbohydrates or polymers. The cells were washed twice in 200 μL cold DPBS/BSA then incubated for 30 min on ice with DTAF-streptavidin (1:100). The cells were again washed twice, then analyzed on a FACSCalibur flow cytometer (BD Biosciences, UT Southwestern Flow Cytometry Core Facility). The background median fluorescence intensity (MFI) for the BSA control sample was subtracted from each sample, and the MFI for the sample with no competitor was normalized to 100 % bound. Averages of 3 independent experiments and their standard deviations are depicted in bar graphs. For analogous detection of lectin binding to Colo205 cells, 50 μL of biotinylated *Aleuria aurantia* lectin (AAL, 10 μg/mL) (Vector Laboratories, catalog no. B-1395), biotinylated *Maackia amurensis* lectin I (MAL I, 40 μg/mL) (Vector Laboratories, catalog no. B-1315), or biotinylated *Sambucus nigra* lectin (SNA, 10 μg/mL) (Vector Laboratories, catalog no. B-1305) were utilized. For free carbohydrate or polymer titration experiments, $IC_{50}$ values were fit to single trials of experimental data using a four-parameter dose-response curve (4PL) within the GraphPad Prism 7 software. $IC_{50}$ values from 3 independent experiments were averaged and reported with their standard deviations.

## ELISA

T84 cells (25,000/well) were cultured in media in individual wells of a collagen-coated 96-well plate (Costar, catalog no. 9102) for 3 d. Cells were washed 2 times in cold DPBS, then 100 μL of various concentrations of biotinylated CTB (0, 1, 4, 10 or 20 μg/mL) (Thermo Fisher Scientific/Invitrogen, catalog no. C-34779) diluted in PBS4+ (PBS with 1 mM $CaCl_2$, 1 mM $MgCl_2$, 0.2% (w/v) BSA, and 5 mM glucose) containing the indicated concentrations

of free carbohydrates were added and the cells incubated for 30 min on ice. Unbound biotinylated CTB was washed away 3 times in cold DPBS. Then cells were fixed with 4 % paraformaldehyde for 5 min on ice and 25 min at room temperature. After 3 washes with DPBS, cells were blocked with 1 % BSA/DPBS. Streptavidin-HRP conjugate (1:10000) was incubated for 1 h to detect biotinylated CTB. HRP activity was measured by a stopped colorimetric assay using ortho-phenylenediamine (OPD) as a substrate. Light absorption at 490 nm was determined with a Synergy Neo microplate reader (BioTek) and all values were corrected by light absorbance at 650 nm and normalized by total cell protein content (bicinchoninic acid assay, Pierce BCA protein assay kit, Pierce). For detection of AAL binding to T84 cells, 100 μL of various concentrations of biotinylated AAL (0, 0.1, 0.4, 1, or 4 μg/mL) was utilized with the indicated concentrations of free carbohydrates. For free carbohydrate or polymer titration experiments, T84 cells were incubated with 50 μL of variable concentrations of the indicated free carbohydrates or polymers in PBS4+ containing 15 μg/mL of biotinylated CTB.

## Isothermal titration calorimetry (ITC)

For ITC experiments, recombinant CTB was produced in-house as described previously. [50] Measurements were performed using a Microcal iTC200 calorimeter (Malvern Instruments), with a sample cell volume of 206 μL and titration syringe of 40 μL. CTB, LeY, and GM1 were diluted in PBS and prior to experiments, and the sample cell was equilibrated with buffer a few minutes. The temperature was set to 25 °C, initial delay 120 s, reference power 6 μCal/s, stirring speed 750 rpm, and high feedback/gain was used. Titrations of 2 μL LeY (concentration range 5–10 mM) to CTB (concentration range 30–40 μM subunits) were performed with 4 s duration, spacing of 240 s and filtering time of 2 s. As a control of the binding activity of CTB, GM1 (100 μM) was titrated to CTB (30 μM subunits) with same titration conditions. For all titration series, a first aliquot of 0.4 μL was injected but not included in the analysis because of uncertainties in concentration of the first distributed volume. After 20 injections, the syringe was refilled, a new 0.4 μL aliquot injected (excluded from analysis) and the titration resumed. The heat change during the titration was registered in real time, and peaks were integrated to obtain the heat change per mole of injectant, ΔQ, for LeY or GM1 using the Origin software (Originlab) supplied with the instrument. Separate titrations of LeY or GM1 into PBS were used to subtract the heat of dilution from the data prior to fitting. A one-site model was used for fitting of the data to obtain the binding constant, $K_D$. The binding stoichiometry (n) was fixed at 1.0 for LeY titrated to CTB, as suggested by Turnbull and Daranas for low c-value titrations.[51]

## Microscale Thermophoresis

CTB labeled with Alexa-488 was purchased from Thermo Fisher Scientific/Invitrogen (catalog no. C22841). The protein was suspended in phosphate-buffered saline (PBS) and centrifuged at 21,100 × *g* for 5 min. The supernatant was used in subsequent experiments. The concentration of the protein was obtained using spectrophotometry coupled with the known extinction coefficient of Alexa-488 and the manufacturer's statement of 60% labeling efficiency. A 400 nM stock solution of CTB was prepared. A 1:1 titration series of LeY in PBS supplemented to 0.1% (v/v) Tween-20 (NanoTemper GmbH, Munich, Germany) was prepared in 10-μL sample volumes; fifteen samples were in the series, which ranged from 20

mM to 1.2 μM. A sixteenth sample having no LeY was included. This titration series was independently prepared in triplicate. An equal volume (10 μL) of labeled CTB stock solution was added to each sample, resulting in a final concentration of CTB of 200 nM and concentrations of 0 to 10 mM of LeY in 0.05% (v/v) Tween-20. After a 45-min incubation at room temperature in the dark, the samples were loaded into standard-treated capillaries (NanoTemper) and inserted into a NanoTemper NT.115 Monolith instrument fitted with the blue filter set. The MST Power was set to 100%, and the LED Power to 50%; the pre-IR, IR-on, and post-IR phases of the experiments were fixed at 5 s, 30 s, and 5 s, respectively. The binding curve was generated in PALMIST;[52] out of 48 data points, five outliers were rejected, followed by averaging of the replicates. The highest-concentration data point was rejected in all three trials because it consistently yielded aberrant thermophoresis. PALMIST's 1:1 binding model was used to analyze the binding curve, with error-surface projection used to determine the 68.3% confidence intervals of the derived parameters. The binding curve was rendered in GUSSI.[53]

### Primary cell data

For experiments with primary cells, recombinant CTB was produced in-house as described previously.[50] Patients undergoing gastric bypass surgery donated human jejunum resections after informed consent. The resected tissue was immediately put in ice-cold Krebs-Ringer solution (118 mM NaCl, 4.69 mM KCl, 2.52 mM CaCl, 1.16 mM $MgSO_4$, 1.01 mM $NaH_2PO_4$, 25 mM $NaHCO_3$ and 12.2 mM D-glucose). After transport, the rest of the mucosa was dissected from the muscle layer, chopped into small pieces and incubated 3 × 15 min at 37 °C in HBSS (without $Ca^{2+}$ and $Mg^{2+}$, Gibco, Thermo Scientific) with 5 mM EDTA, 2 % FBS (Gibco, Thermo Scientific) and 15 mM HEPES (Fisher BioReagents). The mucosa was then washed with HBSS without EDTA for 10 min at 37 °C followed by enzymatic degradation in R10 medium (RPMI1640 (Lonza) with 10 mM HEPES, 10 % FBS, 2 mM L-glutamine, 1 mM sodium pyruvate, 1 % penicillin-streptomycin (Fisher BioReagents) and 10 μg/ml gentamicin (Gibco, Fisher Scientific)) with Liberase-TM and for 45 min at 35 °C. The cell suspension was filtered, washed DNAse I (Roche, Sigma-Aldrich) together with 5 mM $CaCl_2$ and stained with mAbs against EpCAM-FITC, CD45-APC-H7, and with CTB or ovalbumin (OVA) (biotinylated using the kit Lightning-Link® Rapid Biotin, Innova) and streptavidin-BV421 and the live/dead marker Zombie Red (Biolegend). Blocking of CTB binding with LeY and polymers was done as for the cell lines. The cells were then analyzed using flow cytometry as stated previously. The Ethical Review Board, Gothenburg, Sweden, gave ethical approval for acquisition of and experiments on these tissues (jejunal tissue: no 583-17).

## Supplementary Material

Refer to Web version on PubMed Central for supplementary material.

## Acknowledgments

We gratefully acknowledge Michael Lebens (Department of Microbiology and Immunology, University of Gothenburg) for providing recombinant CTB, and Anirudh Sethi (UT Southwestern) for experimental assistance. We acknowledge support from the National Institutes of Health (R01GM090271 to JJK, R01GM097971 to NSS and UY, and R01GM115779 to CSB), Svenska forskningsrådet Formas (68X-22121 to UY), the Welch Foundation

(I-1686 to JJK), The Swedish Research Council (to PW-S), and The Knut and Alice Wallenberg Foundation (to PW-S).

## Abbreviations

| | |
|---|---|
| **2′-FL** | 2′-fucosyllactose |
| **AAL** | *Aleuria aurantia* lectin |
| **B4galnt1** | beta-1,4 N-acetylgalactosaminyltransferase 1 |
| **BGA** | blood group antigen |
| **cAMP** | cyclic adenosine monophosphate |
| **CT** | cholera toxin |
| **CTB** | cholera toxin subunit B |
| **DFL** | difucosyllactose |
| **DTAF** | dichlorotriazinylaminofluorescein |
| **ER** | endoplasmic reticulum |
| **Fuc** | fucose |
| **Gal** | galactose |
| **GalNAc** | N-acetylgalactosamine |
| **GlcNAc** | N-acetylglucosamine |
| **GM1a(os)** | GM1a oligosaccharide |
| **HMO** | human milk oligosaccharide |
| **HRP** | horseradish peroxidase |
| **ITC** | isothermal titration calorimetry |
| **IV** | intravenous |
| **LeY** | Lewis Y |
| **MAL I** | *Maackia amurensis* lectin I |
| **MST** | microscale thermophoresis |
| **OPD** | ortho-phenylenediamine |
| **ORT** | oral rehydration therapy |
| **ROMP** | ring-opening metathesis polymerization |
| **SAR** | structure-activity relationship |

| | |
|---|---|
| **sLeX** | sialyl Lewis X |
| **SNA** | *Sambucus nigra* lectin |

## References


1. Sack DA, Sack RB, Nair GB, Siddique AK. Cholera. Lancet. 2004; 363:223–233. DOI: 10.1016/S0140-6736(03)15328-7 [PubMed: 14738797]
2. Holmgren J, Svennerholm AM. Mechanisms of disease and immunity in cholera: a review. J Infect Dis. 1997; 136(Suppl):S105–S112.
3. Harris JB, LaRocque RC, Qadri F, Ryan ET, Calderwood SB. Cholera. Lancet. 2012; 379:2466–2476. DOI: 10.1016/S0140-6736(12)60436-X [PubMed: 22748592]
4. Wernick NLB, Chinnapen DJF, Cho JA, Lencer WI. Cholera toxin: an intracellular journey into the cytosol by way of the endoplasmic reticulum. Toxins (Basel). 2010; 2:310–325. DOI: 10.3390/toxins2030310 [PubMed: 22069586]
5. Field M. Intestinal ion transport and the pathophysiology of diarrhea. J Clin Invest. 2003; 111:931–943. DOI: 10.1172/JCI18326 [PubMed: 12671039]
6. Merritt EA, Sarfaty S, van den Akker F, L'Hoir C, Martial JA, Hol WG. Crystal structure of cholera toxin B-pentamer bound to receptor GM1 pentasaccharide. Protein Sci. 1994; 3:166–175. DOI: 10.1002/pro.5560030202 [PubMed: 8003954]
7. Turnbull WB, Precious BL, Homans SW. Dissecting the cholera toxin-ganglioside GM1 interaction by isothermal titration calorimetry. J Am Chem Soc. 2004; 126:1047–1054. DOI: 10.1021/ja0378207 [PubMed: 14746472]
8. Holmgren JJ, Lönnroth II, Månsson JJ, Svennerholm LL. Interaction of cholera toxin and membrane GM1 ganglioside of small intestine. Proc Natl Acad Sci U S A. 1975; 72:2520–2524. DOI: 10.1073/pnas.72.7.2520 [PubMed: 1058471]
9. Chinnapen DJF, Hsieh WT, te Welscher YM, Saslowsky DE, Kaoutzani L, Brandsma E, D'Auria L, Park H, Wagner JS, Drake KR, et al. Lipid sorting by ceramide structure from plasma membrane to ER for the cholera toxin receptor ganglioside GM1. Developmental Cell. 2012; 23:573–586. DOI: 10.1016/j.devcel.2012.08.002 [PubMed: 22975326]
10. Saslowsky DE, te Welscher YM, Chinnapen DJF, Wagner JS, Wan J, Kern E, Lencer WI. Ganglioside GM1-mediated transcytosis of cholera toxin bypasses the retrograde pathway and depends on the structure of the ceramide domain. J Biol Chem. 2013; 288:25804–25809. DOI: 10.1074/jbc.M113.474957 [PubMed: 23884419]
11. Cho JA, Chinnapen DJF, Aamar E, te Welscher YM, Lencer WI, Massol R. Insights on the trafficking and retro-translocation of glycosphingolipid-binding bacterial toxins. Front Cell Infect Microbiol. 2012; 2:51.doi: 10.3389/fcimb.2012.00051 [PubMed: 22919642]
12. Yu RK, Usuki S, Itokazu Y, Wu HC. Novel GM1 ganglioside-like peptide mimics prevent the association of cholera toxin to human intestinal epithelial cells in vitro. Glycobiology. 2016; 26:63–73. DOI: 10.1093/glycob/cwv080 [PubMed: 26405107]
13. Branson TR, Turnbull WB. Bacterial toxin inhibitors based on multivalent scaffolds. Chem Soc Rev. 2013; 42:4613–4622. DOI: 10.1039/c2cs35430f [PubMed: 23263178]
14. Zuilhof H. Fighting cholera one-on-one: The development and efficacy of multivalent cholera-toxin-binding molecules. Acc Chem Res. 2016; 49:274–285. DOI: 10.1021/acs.accounts.5b00480 [PubMed: 26760438]
15. Garcia-Hartjes J, Bernardi S, Weijers CAGM, Wennekes T, Gilbert M, Sansone F, Casnati A, Zuilhof H. Picomolar inhibition of cholera toxin by a pentavalent ganglioside GM1os-calix[5]arene. Org Biomol Chem. 2013; 11:4340–4349. DOI: 10.1039/c3ob40515j [PubMed: 23689250]
16. Becker PM, Widjaja-Greefkes HCA, van Wikselaar PG. Inhibition of binding of the AB5-type enterotoxins LT-I and cholera toxin to ganglioside GM1 by galactose-rich dietary components. Foodborne Pathog Dis. 2010; 7:225–233. DOI: 10.1089/fpd.2009.0387 [PubMed: 19919285]

17. Pukin AV, Branderhorst HM, Sisu C, Weijers CAGM, Gilbert M, Liskamp RMJ, Visser GM, Zuilhof H, Pieters RJ. Strong inhibition of cholera toxin by multivalent GM1 derivatives. Chembiochem. 2007; 8:1500–1503. DOI: 10.1002/cbic.200700266 [PubMed: 17625801]
18. Branderhorst HM, Liskamp RMJ, Visser GM, Pieters RJ. Strong inhibition of cholera toxin binding by galactose dendrimers. Chem Commun (Camb). 2007; 81:5043–5045. DOI: 10.1039/b711070g
19. Tran HA, Kitov PI, Paszkiewicz E, Sadowska JM, Bundle DR. Multifunctional multivalency: a focused library of polymeric cholera toxin antagonists. Org Biomol Chem. 2011; 9:3658–3671. DOI: 10.1039/c0ob01089h [PubMed: 21451844]
20. Richards SJ, Jones MW, Hunaban M, Haddleton DM, Gibson MI. Probing bacterial-toxin Inhibition with synthetic glycopolymers prepared by tandem post-polymerization modification: Role of linker length and carbohydrate density. Angew Chem Int Ed Engl. 2012; 51:7812–7816. DOI: 10.1002/anie.201202945 [PubMed: 22715146]
21. Zomer-van Ommen DD, Pukin AV, Fu O, Quarles van Ufford LHC, Janssens HM, Beekman JM, Pieters RJ. Functional characterization of cholera toxin inhibitors using human intestinal organoids. J Med Chem. 2016; 59:6968–6972. DOI: 10.1021/acs.jmedchem.6b00770 [PubMed: 27347611]
22. Breimer ME, Hansson GC, Karlsson KA, Larson G, Leffler H. Glycosphingolipid composition of epithelial cells isolated along the villus axis of small intestine of a single human individual. Glycobiology. 2012; 22:1721–1730. DOI: 10.1093/glycob/cws115 [PubMed: 22833314]
23. Cervin J, Wands AM, Casselbrant A, Wu H, Krishnamurthy S, Cvjetkovic A, Estelius J, Dedic B, Sethi A, Wallom K-L, et al. GM1 ganglioside-independent intoxication by cholera toxin. PLoS Pathog. in press.
24. Mandal PK, Branson TR, Hayes ED, Ross JF, Gavín JA, Daranas AH, Turnbull WB. Towards a structural basis for the relationship between blood group and the severity of El Tor cholera. Angew Chem Int Ed Engl. 2012; 51:5143–5146. DOI: 10.1002/anie.201109068 [PubMed: 22488789]
25. Heggelund JE, Burschowsky D, Bjørnestad VA, Hodnik V, Anderluh G, Krengel U. High-resolution crystal structures elucidate the molecular basis of cholera blood group dependence. PLoS Pathog. 12:e1005567.
26. Vasile F, Reina JJ, Potenza D, Heggelund JE, Mackenzie A, Krengel U, Bernardi A. Comprehensive analysis of blood group antigen binding to classical and El Tor cholera toxin B-pentamers by NMR. Glycobiology. 2014; 24:766–778. DOI: 10.1093/glycob/cwu040 [PubMed: 24829308]
27. El-Hawiet A, Kitova EN, Klassen JS. Recognition of human milk oligosaccharides by bacterial exotoxins. Glycobiology. 2015; 25:845–854. DOI: 10.1093/glycob/cwv025 [PubMed: 25941008]
28. Karki G, Mishra VN, Mandal PK. An expeditious synthesis of blood-group antigens, ABO histo-blood group type II antigens and xenoantigen oligosaccharides with amino type spacer–arms. Glycoconj J. 2016; 33:63–78. DOI: 10.1007/s10719-015-9635-1 [PubMed: 26572140]
29. Prudden AR, Liu L, Capicciotti CJ, Wolfert MA, Wang S, Gao Z, Meng L, Moremen KW, Boons GJ. Synthesis of asymmetrical multiantennary human milk oligosaccharides. Proc Natl Acad Sci U S A. 2017; 114:6954–6959. DOI: 10.1073/pnas.1701785114 [PubMed: 28630345]
30. Wands AM, Fujita A, McCombs JE, Cervin J, Dedic B, Rodriguez AC, Nischan N, Bond MR, Mettlen M, Trudgian DC, et al. Fucosylation and protein glycosylation create functional receptors for cholera toxin. eLife. 2015; 4:e09545.doi: 10.7554/eLife.09545 [PubMed: 26512888]
31. O'Hagan D. Understanding organofluorine chemistry. An introduction to the C–F bond. Chem Soc Rev. 2008; 37:308–319. DOI: 10.1039/b711844a [PubMed: 18197347]
32. Lindhorst TK, Thiem J. The synthesis of 3-deoxy-L-fucose (3,6-dideoxy-L-xylo-hexose). Liebigs Annalen der Chemie. 1990; 1990:1237–1241. DOI: 10.1002/jlac.1990199001222
33. Morrow AL, Ruiz-Palacios GM, Altaye M, Jiang X, Guerrero ML, Meinzen-Derr JK, Farkas T, Chaturvedi P, Pickering LK, Newburg DS. Human milk oligosaccharides are associated with protection against diarrhea in breast-fed infants. J Pediatr. 2004; 145:297–303. DOI: 10.1016/j.jpeds.2004.04.054 [PubMed: 15343178]

34. Newburg DS, Ruiz-Palacios GM, Morrow AL. Human milk glycans protect infants against enteric pathogens. Annu Rev Nutr. 2005; 25:37–58. DOI: 10.1146/annurev.nutr.25.050304.092553 [PubMed: 16011458]
35. Lesieur C, Cliff MJ, Carter R, James RFL, Clarke AR, Hirst TR. A kinetic model of intermediate formation during assembly of cholera toxin B-subunit pentamers. J Biol Chem. 2002; 277:16697–16704. DOI: 10.1074/jbc.M110561200 [PubMed: 11877421]
36. Jones GW, Freter R. Adhesive properties of Vibrio cholerae: nature of the interaction with isolated rabbit brush border membranes and human erythrocytes. Infect Immun. 1976; 14:240–245. [PubMed: 985805]
37. Barua D, Paguio AS. ABO blood groups and cholera. Ann Hum Biol. 1977; 4:489–492. DOI: 10.1080/03014467700002481 [PubMed: 603230]
38. Yamamoto F. Cloning and regulation of the ABO genes. Transfusion Medicine. 2001; 11:281–294. DOI: 10.1046/j.1365-3148.2001.00316.x [PubMed: 11532185]
39. Kunz, C., Kuntz, S., Rudloff, S. Production, Analysis and Bioactivity. Vol. 346. John Wiley & Sons, Ltd; Chichester, UK: 2014. Bioactivity of Human Milk Oligosaccharides; p. 1-20.
40. Castanys-Muñoz E, Martin MJ, Prieto PA. 2′-fucosyllactose: An abundant, genetically determined soluble glycan present in human milk. Nutrition Reviews. 2013; 71:773–789. DOI: 10.1111/nure.12079 [PubMed: 24246032]
41. Bode L. Human milk oligosaccharides: Every baby needs a sugar mama. Glycobiology. 2012; 22:1147–1162. DOI: 10.1093/glycob/cws074 [PubMed: 22513036]
42. Mudrak B, Kuehn MJ. Heat-labile enterotoxin: Beyond GM1 binding. Toxins (Basel). 2010; 2:1445–1470. DOI: 10.3390/toxins2061445 [PubMed: 22069646]
43. Morita A, Tsao D, Kim YS. Identification of cholera toxin binding glycoproteins in rat intestinal microvillus membranes. J Biol Chem. 1980; 255:2549–2553. [PubMed: 7358687]
44. Monferran CG, Roth GA, Cumar FA. Inhibition of cholera toxin binding to membrane receptors by pig gastric mucin-derived glycopeptides: differential effect depending on the ABO blood group antigenic determinants. Infect Immun. 1990; 58:3966–3972. [PubMed: 1701416]
45. Platt FM, Reinkensmeier G, Dwek RA. Extensive glycosphingolipid depletion in the liver and lymphoid organs of mice treated with N-butyldeoxynojirimycin. J Biol Chem. 1997; 272:19365–19372. DOI: 10.1074/jbc.272.31.19365 [PubMed: 9235935]
46. Hansen GH, Dalskov SM, Rasmussen CR, Immerdal L, Niels-Christiansen LL, Danielsen EM. Cholera toxin entry into pig enterocytes occurs via a lipid raft- and clathrin-dependent mechanism. Biochemistry. 2005; 44:873–882. DOI: 10.1021/bi047959 [PubMed: 15654743]
47. Yanagisawa M, Ariga T, Yu RK. Cholera toxin B subunit binding does not correlate with GM1 expression: a study using mouse embryonic neural precursor cells. Glycobiology. 2006; 16:19G–22G. DOI: 10.1093/glycob/cwl003
48. Blank N, Schiller M, Krienke S, Wabnitz G, Ho AD, Lorenz HM. Cholera toxin binds to lipid rafts but has a limited specificity for ganglioside GM1. Immunol Cell Biol. 2007; 85:378–382. DOI: 10.1038/sj.icb.7100045 [PubMed: 17325693]
49. Day CA, Kenworthy AK. Mechanisms underlying the confined diffusion of cholera toxin B-subunit in intact cell membranes. PLoS ONE. 2012; 7:e34923.doi: 10.1371/journal.pone.0034923 [PubMed: 22511973]
50. Lebens M, Johansson S, Osek J, Lindblad M. Large-scale production of Vibrio cholerae toxin B subunit for use in oral vaccines. Bio/Technology. 1993; 11:1574–1578. DOI: 10.1038/nbt1293-1574 [PubMed: 7764248]
51. Turnbull WB, Daranas AH. On the value of c: can low affinity systems be studied by isothermal titration calorimetry? J Am Chem Soc. 2003; 125:14859–14866. DOI: 10.1021/ja036166s [PubMed: 14640663]
52. Scheuermann TH, Padrick SB, Gardner KH, Brautigam CA. On the acquisition and analysis of microscale thermophoresis data. Anal Biochem. 2016; 496:79–93. DOI: 10.1016/j.ab.2015.12.013 [PubMed: 26739938]
53. Brautigam CA. Calculations and publication-quality illustrations for analytical ultracentrifugation data. Meth Enzymol. 2015; 562:109–133. DOI: 10.1016/bs.mie.2015.05.001 [PubMed: 26412649]

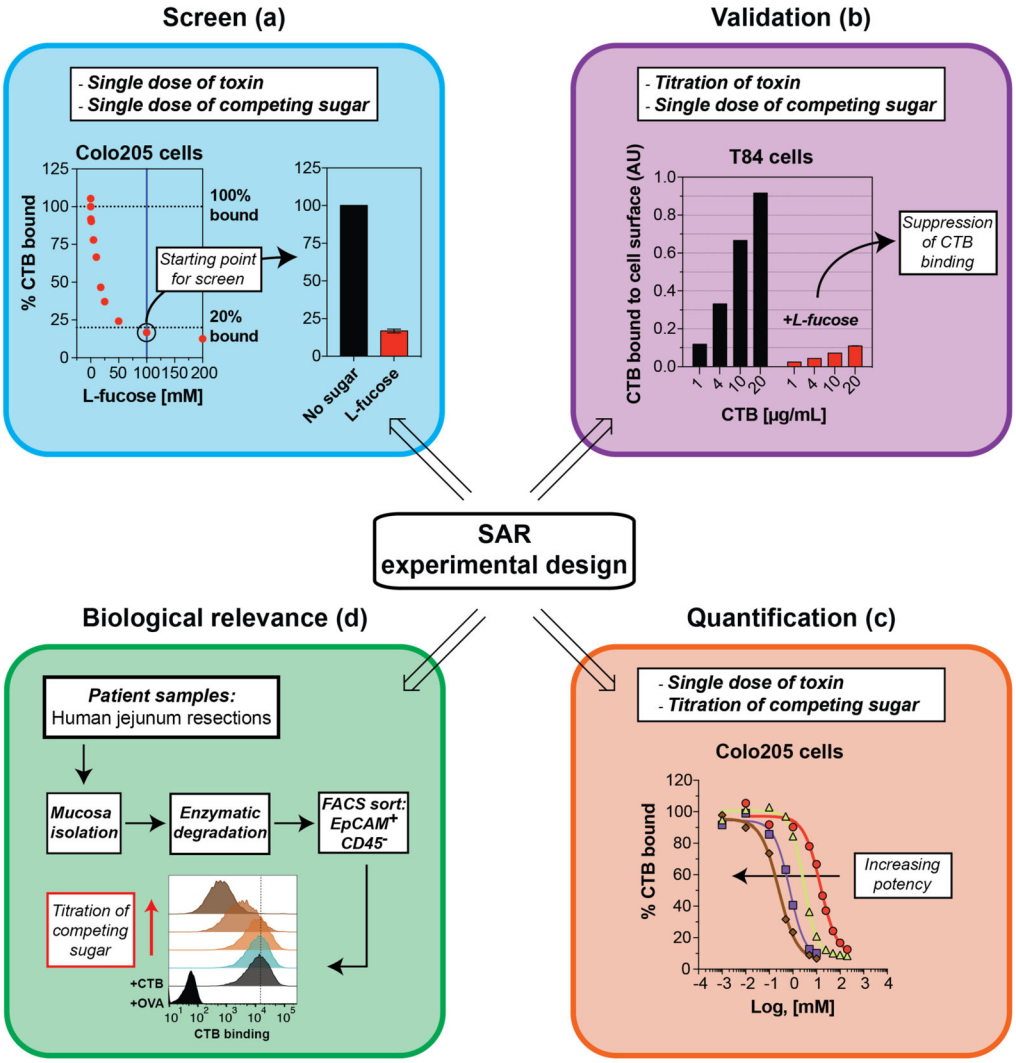


**Figure 1. Experimental strategy to discover fucose-based inhibitors of CTB cell surface binding**

Step-wise approaches employed in this work to identify L-fucose based inhibitors of CTB binding. (**a**) Candidate inhibitors were first screened at a single dose of toxin and single dose of inhibitor against Colo205 cells to identify structural changes that reduce or increase inhibitory effectiveness. (**b**) The generality of these results was evaluated using T84 cells and titrating the CTB concentration. (**c**) For a select subset of inhibitors, quantitative comparison (*i.e.* IC50 determination) was achieved by titrating the inhibitor concentration and measuring CTB binding to Colo205 cells by flow cytometry. (**d**) The most potent inhibitors were tested for their ability to block CTB binding to the physiological target, human jejunal primary epithelial cells.

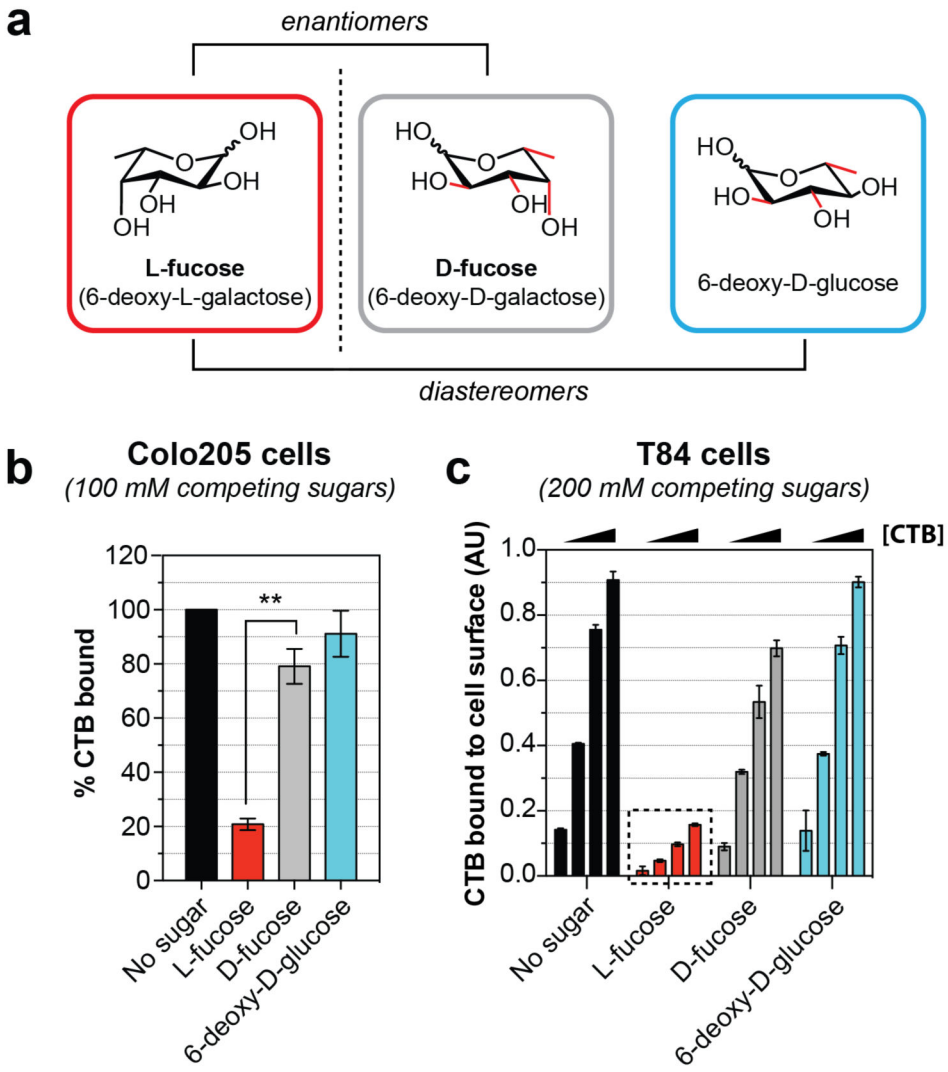


**Figure 2. Stereochemical requirements for fucose inhibition of CTB binding to cell surfaces**

(**a**) Stereoisomers of L-fucose used in this study. (**b**) Inhibition of CTB binding to Colo205 cells in a flow cytometry assay. Error bars represent the standard deviation from the mean (n = 3). Histograms for a single representative trial are presented in Figure S2. Statistical significance determined by unpaired Welch's test: ** indicates a $p$ value < 0.01. (**c**) Inhibition of CTB binding to T84 cells as measured by ELISA. Error bars represent the standard deviation from the mean (n = 2).

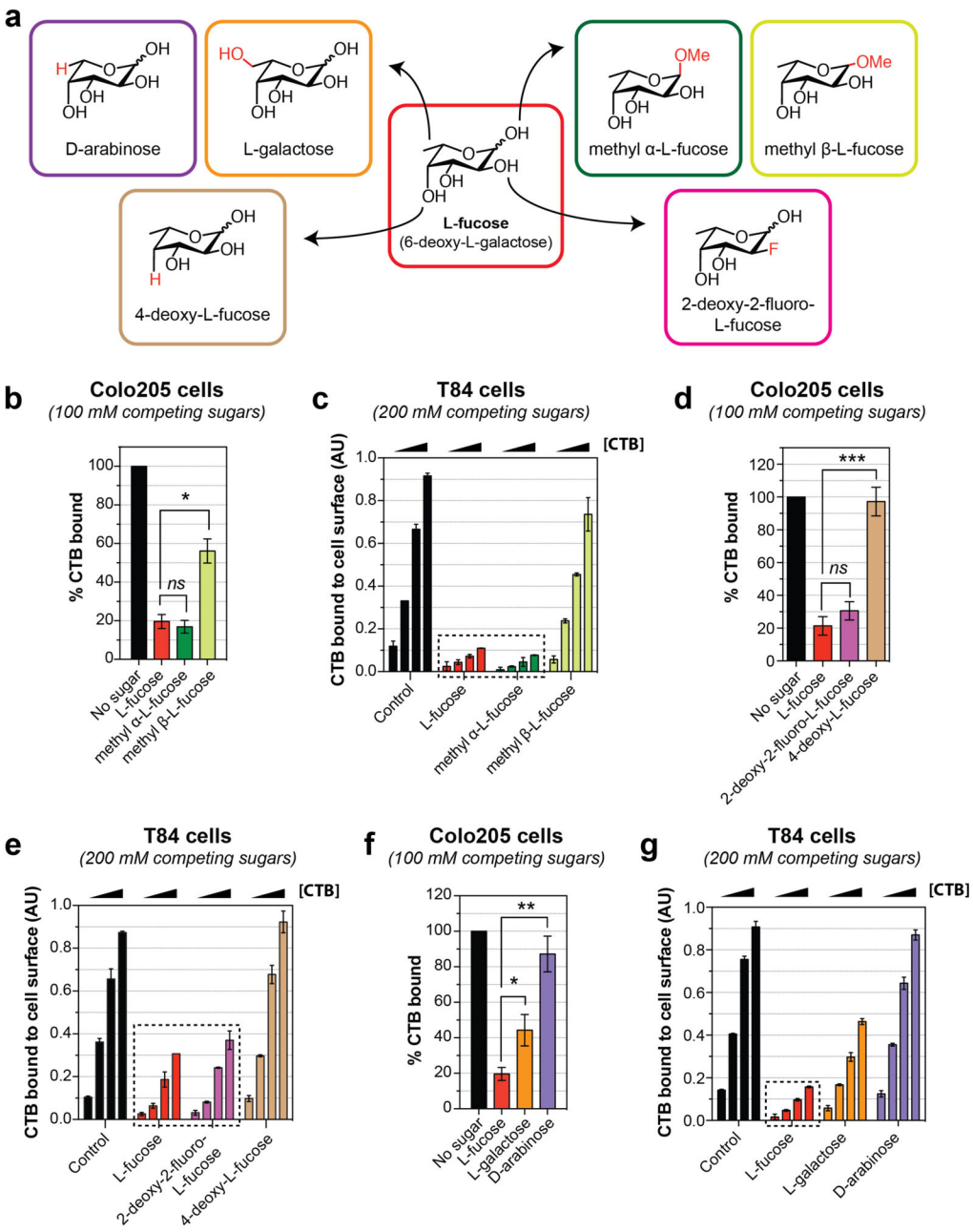


**Figure 3. Structure-activity relationship (SAR) analysis of fucose inhibition of CTB binding to cell surfaces**

(**a**) Positional analogs of L-fucose used in this study. (**b**, **d**, and **f**) Inhibition of CTB binding to Colo205 cells in a flow cytometry assay. Monosaccharides vary from L-fucose at positions 1 (**b**), positions 2 and 4 (**d**), and positions 5 and 6 (**f**). Error bars represent the standard deviation from the mean (n = 3). Histograms for a single representative trial are presented in Figure S3. Statistical significance determined by unpaired Welch's test: *** indicates a $p$ value < 0.001, ** indicates a $p$ value < 0.01, and * indicates a $p$ value < 0.05. *ns* indicates difference not statistically significant. (**c**, **e**, and **g**) Inhibition of CTB binding to T84 cells as measured by ELISA. Monosaccharides vary from L-fucose at positions 1 (**c**),

positions 2 and 4 (**e**), and positions 5 and 6 (**g**). Error bars represent the standard deviation from the mean (n = 2).

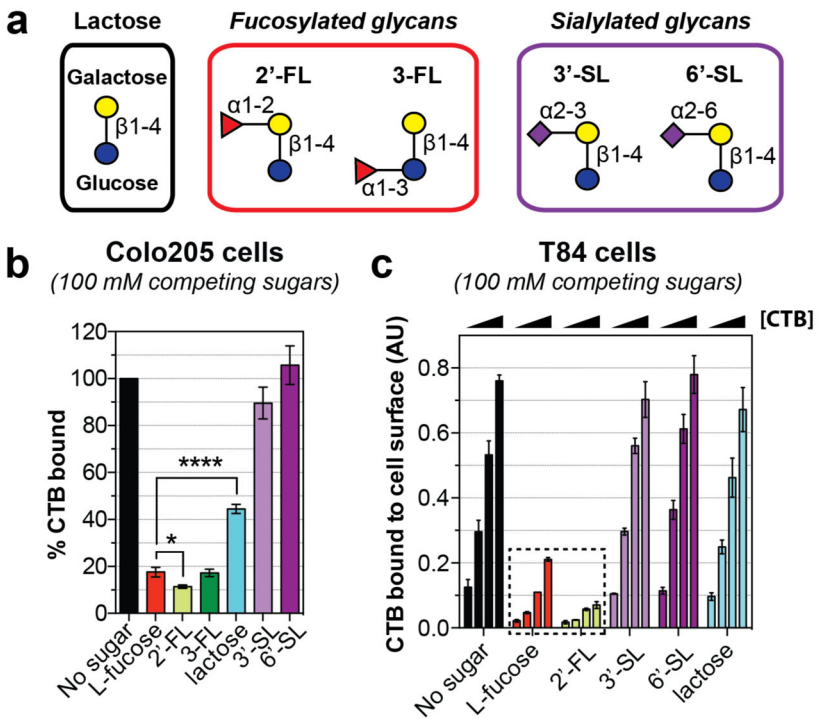


**Figure 4. HMOs can competitively inhibit CTB binding to cell surfaces**

(**a**) Human milk oligosaccharides (HMOs) used in this study. (**b**) Inhibition of CTB binding to Colo205 cells measured by flow cytometry. Error bars represent the standard deviation from the mean (n = 3). Histograms for a single representative trial are presented in Figure S8. Statistical significance determined by unpaired Welch's test: **** indicates a $p$ value < 0.0001 and * indicates a $p$ value < 0.05. (**c**) Inhibition of CTB binding to T84 cells measured by ELISA. Error bars represent the standard deviation from the mean (n = 2).

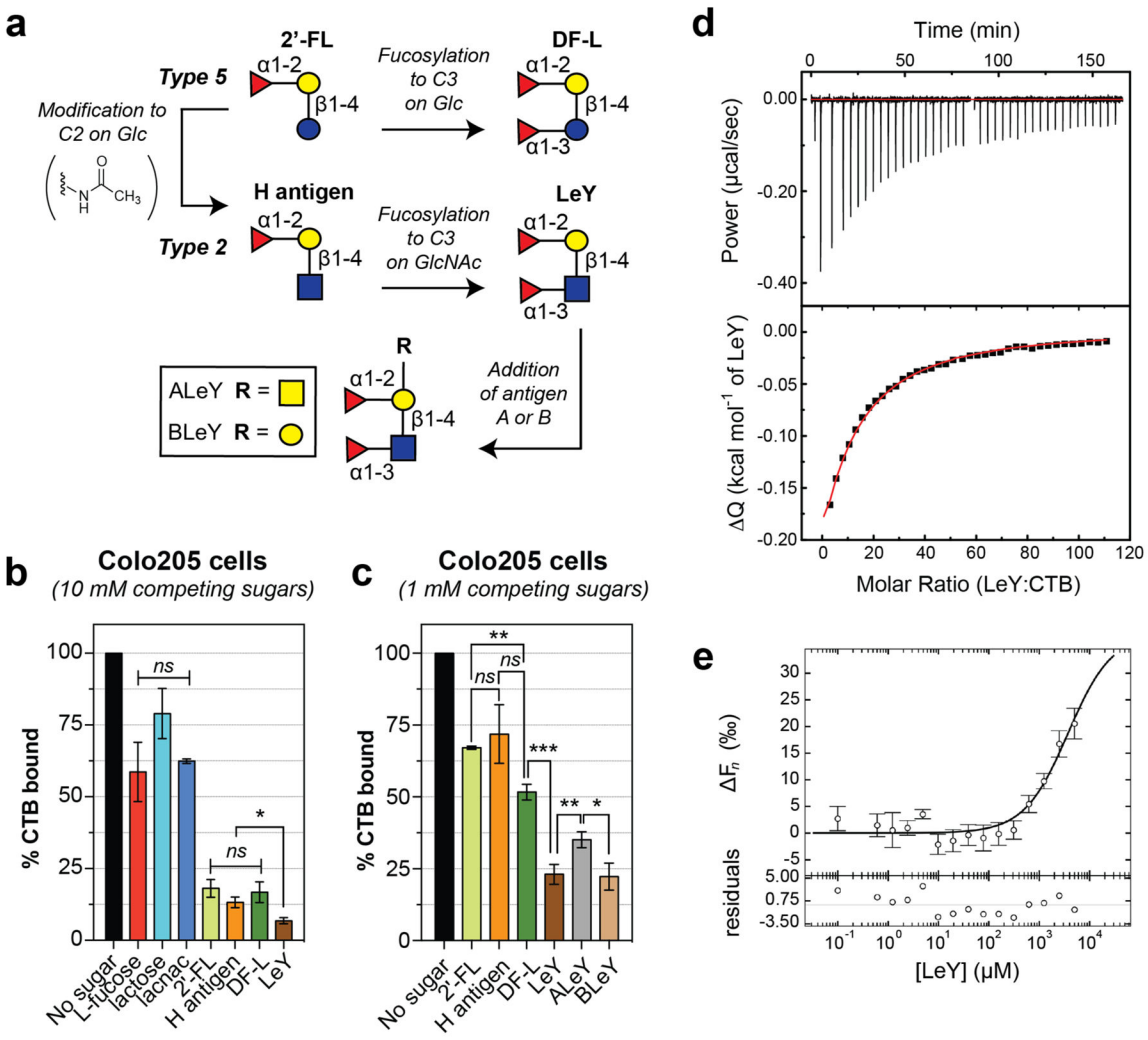


**Figure 5. A difucosylated glycan, LeY, emerges as a more potent inhibitor of CTB binding**

(**a**) Stepwise conversion of 2′-FL to LeY. (**b** and **c**) Inhibition of CTB binding to Colo205 cells in a flow cytometry assay with 10 mM (**b**) and 1 mM (**c**) competing sugars. Error bars represent the standard deviation from the mean (n = 3). Histograms for a single representative trial are presented in Figure S11. Statistical significance determined by unpaired Welch's test: *** indicates a $p$ value < 0.001, ** indicates a $p$ value < 0.01, and * indicates a $p$ value < 0.05. *ns* indicates difference not statistically significant. (**d**) ITC measurement of 10 mM LeY titrated to 40 μM CTB in PBS pH 7.4. Top panel represents the power recorded during titration and bottom panel the heats per mol LeY obtained by integration of the peaks and subtraction of the heat of dilution for LeY titrated to PBS The data was fitted with a one-site model (red line) assuming 1:1 binding (see Table S3 for details). (**e**) MST of LeY binding to CTB. In the upper panel, the thermophoresis ("$\Delta F_n$") values were baseline-corrected by subtracting the refined value of the thermophoresis for the unbound CTB. Circles represent the means of three replicates except for the 4.9 μM and 312.5 μM samples, which were replicated only twice. Error bars are the respective standard

deviations of the means. The black line is a fit to the data with a 1:1 binding model. The circles in the lower panel show the residuals between the data points and the fit line.

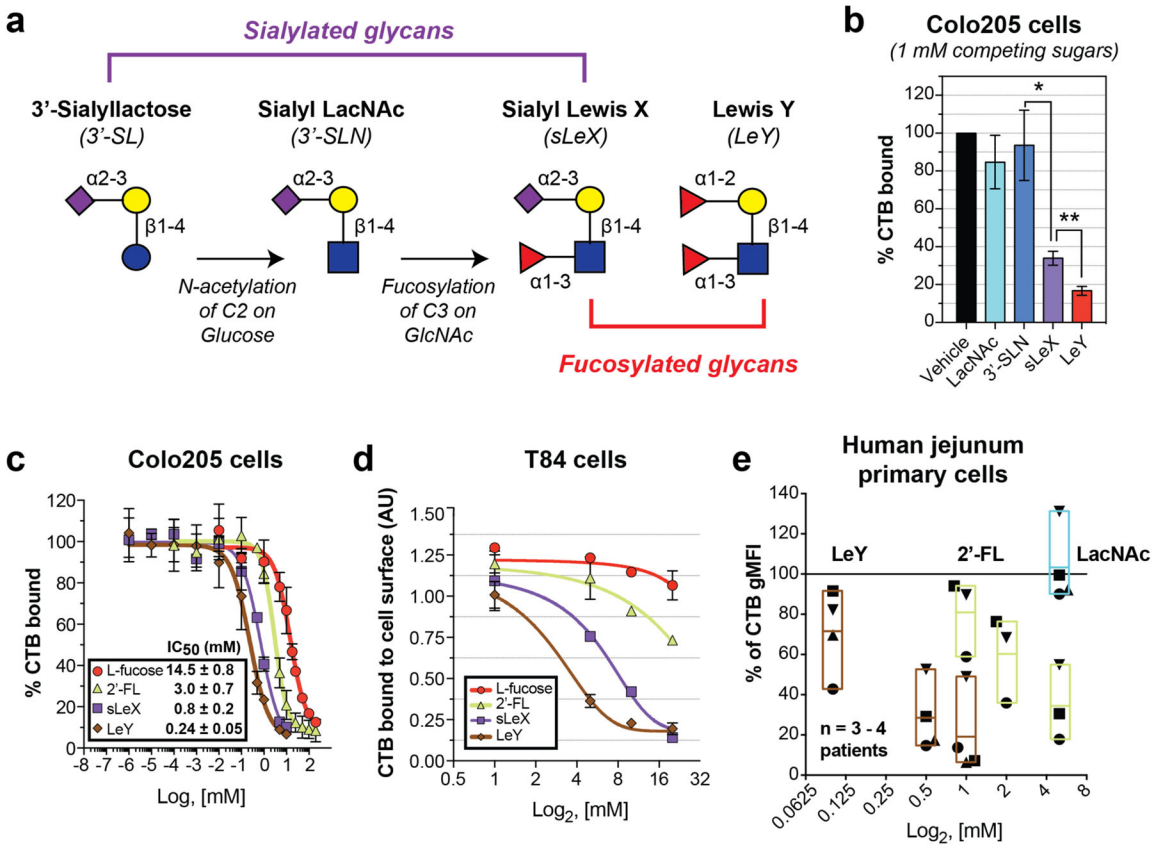


**Figure 6. Comparison of the inhibitory potential of sialylated and fucosylated ligands for CTB**

(**a**) Conversion of an inactive ligand (3′-SL) into a CTB inhibitor (sLeX). (**b**) Inhibition of CTB binding to Colo205 cells in a flow cytometry assay. Error bars represent the standard deviation from the mean (n = 3). Histograms for a single representative trial are presented in Figure S15. Statistical significance determined by unpaired Welch's test: ** indicates a *p* value < 0.01, and * indicates a *p* value < 0.05. (**c**) Dose-dependent inhibition of CTB binding to Colo205 cells in a flow cytometry assay. Error bars represent the standard deviation from the mean (n = 3). $IC_{50}$ values were calculated for individual replicates using GraphPad Prism software and then averaged. (**d**) Dose-dependent inhibition of CTB binding to T84 cells measured by ELISA. Error bars represent the standard deviation from the mean (n = 2). (**e**) Inhibition of CTB binding to freshly isolated human jejunal epithelial cells (EpCAM+, CD45 negative) in a flow cytometry assay. Data points indicate % of unblocked CTB gMFI, with unique symbols indicating single patients (n = 3 – 4 patients). Box plots encompassing low-high data points indicate the mean value with an internal line. Flow cytometry histograms for cells from a single representative patient are presented in Figure S17.

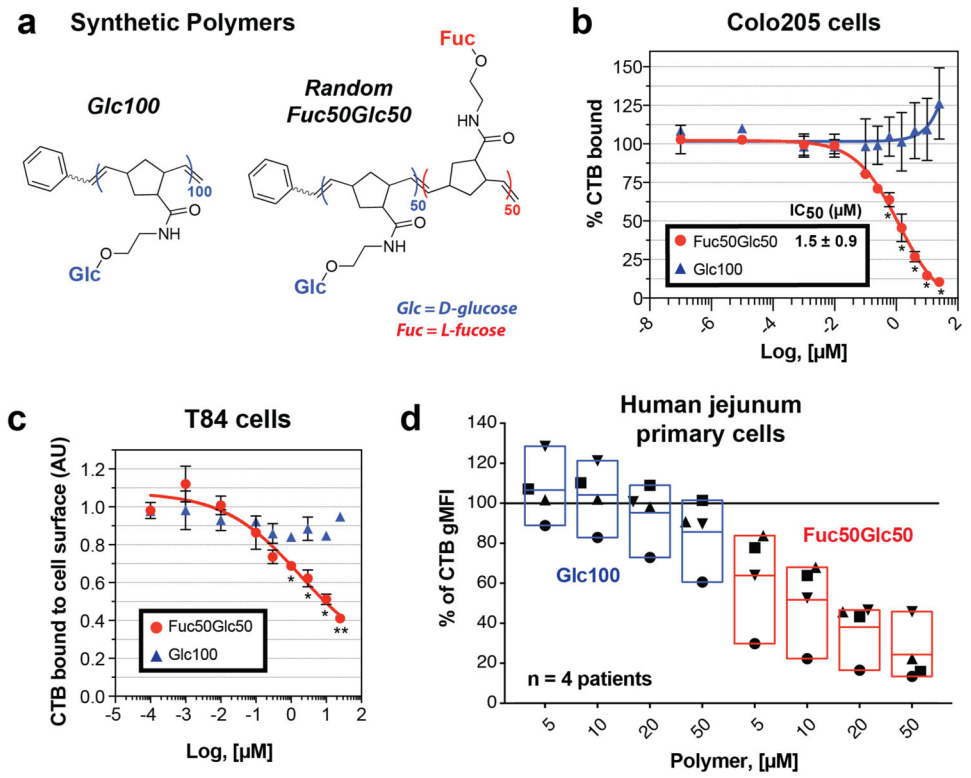


**Figure 7. Fucose-containing polymers block CTB binding to intestinal epithelial cell lines**

(**a**) Synthetic fucose- and glucose-containing polymers used in this study. (**b**) Dose-dependent inhibition of CTB binding to Colo205 cells in a flow cytometry assay. Error bars represent the standard deviation from the mean (n = 3). $IC_{50}$ values were calculated for individual replicates using GraphPad Prism software and then averaged. (**c**) Dose-dependent inhibition of CTB binding to T84 cells measured by ELISA. Error bars represent the standard deviation from the mean (n = 2). Statistical significance determined by unpaired Welch's test: *** indicates a *p* value < 0.001, ** indicates a *p* value < 0.01 and * indicates a *p* value < 0.05. (**d**) Inhibition of CTB binding to freshly isolated human jejunal epithelial cells (EpCAM+, CD45 negative) in a flow cytometry assay. Data points indicate % of unblocked CTB gMFI, with unique symbols indicating single patients (n = 4 patients). Box plots encompassing low-high data points indicate the mean value with an internal line. Flow cytometry histograms for cells from a single representative patient are presented in Figure S20.